

Experimental Evaluation and Computer Analysis of Multi-Spiral Confinement in Reinforced Concrete Columns

by

Briana K. Brubaker

B.S., Kansas State University, 2011

A Report

submitted in partial fulfillment of the requirements for the degree

Master of Science

Department of Civil Engineering
College of Engineering

Kansas State University
Manhattan, Kansas

2017

Approved by:

Major Professor
Dr. Asad Esmaily

COPYRIGHT

Briana K. Brubaker

2017

ABSTRACT

Bridge and building construction in areas that sustain frequent seismic activity require the use of heavy lateral steel reinforcement within concrete columns to handle the lateral loads. Multi-spiral lateral reinforcement has been recently introduced to the construction field to offer an alternative to the traditional hoop and tie reinforcement. This report evaluates the experimental data observed in multiple experimental studies done on different concrete specimens. These specimens include multiple rectilinear reinforcement and several multi-spiral configurations in both rectangular and oblong columns. Due to multi-spiral reinforcement being a relatively new design, traditional computer programs have yet to include design analysis for this type of reinforcement in computer programs. Dr. Asad Esmaily developed the program KSU RC 2.0 that can implement multiple analytical models to evaluate different multi-spiral configurations, as well as traditional hoop and tie confinement, that may be compared with experimental data. This report illustrates the comparative data from several different reinforced concrete column models. The data clearly indicates that multi-spiral reinforced columns exhibit higher compressive strength in the axial direction as well as higher ductility capabilities when compared to traditional rectilinear reinforcement of similar lateral steel reinforcement ratios. The use of multi-spiral reinforcement is also shown to lower costs for both the work time needed to install the structures as well as lowering the required steel ratio; all while maintaining the structural integrity of the columns.

TABLE OF CONTENTS

List of Figures	vi
List of Tables	vii
Acknowledgements	viii
Dedication	ix
1. Introduction	1
<i>1.1 Seismic Background</i>	<i>1</i>
<i>1.2 Construction</i>	<i>1</i>
<i>1.3 Spiral Reinforcement Design</i>	<i>2</i>
<i>1.4 Multi-Spiral Analysis</i>	<i>4</i>
<i>1.5 Objectives</i>	<i>4</i>
2. Codes & Requirements	4
<i>2.1 Transverse Reinforcement</i>	<i>4</i>
<i>2.2 Axial Force-Moment Interaction</i>	<i>6</i>
3. Specimens	7
<i>3.1 Experimental Configurations</i>	<i>7</i>
3.1.1 Square Columns	7
3.1.2 Rectangular Columns	8
3.1.3 Oblong Columns	10
<i>3.2 Computer Analyzed Layouts</i>	<i>11</i>
<i>3.3 Material Properties</i>	<i>13</i>
4. Testing Setup	16
<i>4.1 Axial Compressive Loading</i>	<i>16</i>
<i>4.2 Combined Axial and Lateral Cyclic Loading</i>	<i>17</i>
<i>4.3 Computer Cross-sections</i>	<i>19</i>
5. Test Results	20
<i>5.1 Axial Results</i>	<i>20</i>
<i>5.2 Combined Axial and Cyclic Load Results</i>	<i>23</i>
<i>5.3 Computer Program Analysis</i>	<i>26</i>
6. Experimental & Computer Analysis Comparison	29

6.1 Axial Stress – Bending Moment.....	29
6.2 Lateral Forces	29
7. Conclusions and Recommendations	30
7.1 Experimental Data.....	30
7.2 KSU RC 2.0.....	30
7.3 Recommendations	31
7.3.1 Multi-Spiral Reinforcement	31
7.3.2 Computer Software	31
References	32

LIST OF FIGURES

Figure 1: 5-Spiral and 4-Spiral Configurations	2
Figure 2: 6-Spiral Configuration.....	3
Figure 3: Oblong Double Spiral Configuration	3
Figure 4: Transverse Reinforcement Configurations for Square Columns	8
Figure 5: Transverse Reinforcement Configurations for Rectangular Columns	9
Figure 6: Transverse Reinforcement Configurations for Oblong Columns.....	10
Figure 7: Computer Programmed Transverse Reinforcement Configurations.....	12
Figure 8: Axial Test Setup (Yin, Wang and Wang 2012).....	16
Figure 9: Lateral Hydraulic Jack (Ou, et al. 2015).....	17
Figure 10: Lateral Hydraulic Jack and LVDT (Hung, et al. 2012).....	18
Figure 11: Axial Failure Examples (Yin, Wang and Wang 2012)	20
Figure 12: Axial Stress - Strain Diagram.....	21
Figure 13: Axial Failure Examples (Ou, et al. 2015).....	23
Figure 14: Hysteresis Envelopes.....	25
Figure 15: Axial Stress - Moment Computer Model Diagram (Including Experimental Results for two of the cross-sections).....	26
Figure 16: Lateral Stress - Deflection Diagram.....	27
Figure 17 - Moment - Curvature Diagram.....	28

LIST OF TABLES

Table 1: Material Properties I	14
Table 2: Material Properties II	15
Table 3: Steel Reduction Ratios.....	22

ACKNOWLEDGEMENTS

I would first and foremost like to extend my deepest gratitude to my Primary Advisory and Committee Chair Dr. Asad Esmaily. It is greatly due to his patient guidance that I have been able to complete my coursework as both an undergraduate student as well as Master's student. I would like to thank the Interim Department Head of the Civil Engineering Department, and committee member, Dr. Robert Stokes for his continuous help throughout the duration of my education. I would also like to thank Dr. Hani Melhem for agreeing to be a part of this committee on such short notice. To all my wonderful teachers I would also like to extend my appreciation for their continuous efforts.

Thanks are also due to the wonderful ladies of the Civil Engineering Department office. Sue Wells and Jayme Reid are some of the unsung heroes of the university system.

Lastly I would like to thank my friends and family. Without their constant help and support I would not have been able to finish this degree.

DEDICATION

Danielle, this is for you kid.

1. INTRODUCTION

1.1 SEISMIC BACKGROUND

Concrete bridge columns in seismic areas are subjected to varying loading combinations including axial, flexural, shear and torsional forces. This combination of loading requires a significant amount of transverse reinforcement. Traditional transverse reinforcement in reinforced concrete columns consists of perimeter hoops and cross ties. This reinforcement provides a combination of benefits for the strength of the column. Lateral reinforcement provides a passive confinement effect that increases the ultimate axial load. Confinement steel also provides columns with higher shear strength capacities as well as an increase in ductility.

Traditional rectilinear reinforcement does come with a set of problems unique to rectangular shaped columns. Conventional reinforcement performs poorly in distributing the lateral stresses owing to the uneven nature of the layout of the lateral steel. Due to the extreme need for ductility and shear transfer in highly seismic areas, the amount of traditional rectilinear reinforcement can cause significant congestion. Another concerning issue with high lateral reinforcement designs is the additional time needed to form, install, and tie each perimeter hoop for each column.

1.2 CONSTRUCTION

One of the largest goals in construction, especially in the most recent years, is streamlining the construction process while continuing to improve the quality of structures. The market is very competitive and prefabricated technologies are saturating this market. These automated processes are allowing those who work in the construction industry to produce high quality products quicker and with fewer errors. This construction technology includes the production of spiral lateral reinforcement for structural columns. While traditional hoop and tie reinforcement requires on-site bending formation and tying, spiral reinforcement can be placed much quicker. These spiral reinforcement alternatives can reduce time and labor while improving the overall quality of the final product. However, due to the difference in shape between the majority of bridge columns (rectangular) and spiral reinforcement (circular), finding adequate configurations can be problematic.

1.3 SPIRAL REINFORCEMENT DESIGN

The use of spiral reinforcement of circular columns has been widely experimented and investigated. Spiral reinforcement has continually shown higher ductility due to the ability to transfer the lateral forces into longitudinal elongation. This has been investigated by Kupfer, Hilsdorf, & Rusch 1969, Mander, Priestly, & Park 1988, Ahmad & Shah 1982, Darwin & Pecknold 1969, Shah, Fafitis, & Arnold 1983, Sheikh & Toklucu 1993, Tanaka & Park 1999, Pantazopoulou 1998.

The strength of spiral reinforcement versus traditional reinforcement has been shown to perform at an increased amount of 10%. The ratio of steel required for confinement can also be reduced by as much as 30% (Yin, Wang and Wang 2012). Recent investigations have gone into harnessing the benefits of spiral reinforcement in non-conforming shaped columns such as rectangles and oblong shapes.

The use of spiral lateral reinforcement in a rectangular column would potentially leave a large amount of unconfined concrete. This would negate the additional benefits of replacing the traditional hoop and tie reinforcement with spiral reinforcement. However, (Yin et al. 2004) developed an innovated multi-spiral reinforcement scheme that would more completely confine the core concrete while provided stabilizing lateral reinforcement for the longitudinal bars. These lateral spiral designs are referred to as the 5-spiral and the 4-spiral as shown in Figure 1. The amount, size, and location of longitudinal reinforcement can widely vary between each design. Different longitudinal rebar locations are illustrated later in this paper.

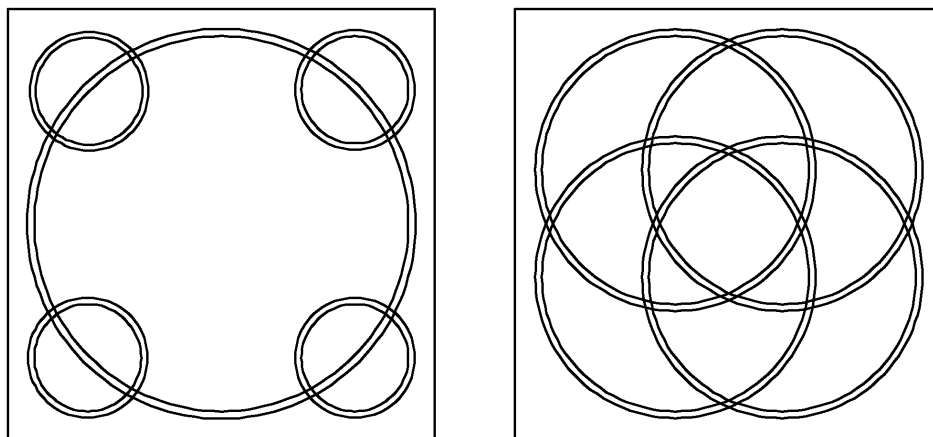


Figure 1: 5-Spiral and 4-Spiral Configurations

These interlocking spiral layouts address square columns, but do not adequately cover rectangular columns with one side significantly longer than the other. This layout issue has been addressed with several different options, but most notably by extending the 5-spiral design to include a second large center hoop (Huy 2012), (Hung, et al. 2012). This basic layout is illustrated in Figure 2. As with the previous layouts, the type of longitudinal reinforcement varies. Further configurations have also been included and will be listed further in this paper.

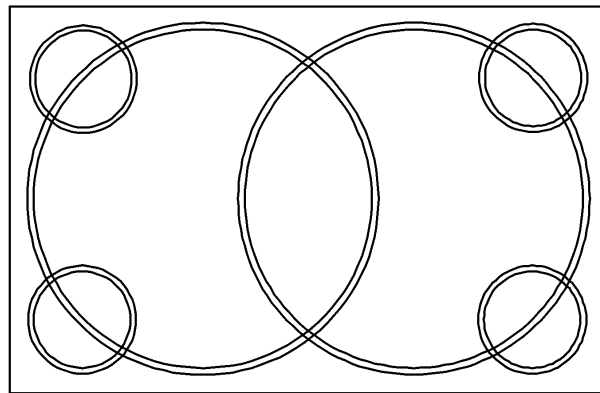


Figure 2: 6-Spiral Configuration

Along with rectangular and square shaped columns, oblong columns have also been included in these recent studies for spiral lateral reinforcement. Tanaka and Park's (1993) study on multi-spiral reinforcement included oblong columns with a configuration containing two interlocking spirals as shown in Figure 3. Longitudinal reinforcement bar configurations can vary between each study and will be shown as they are for the test specimens.

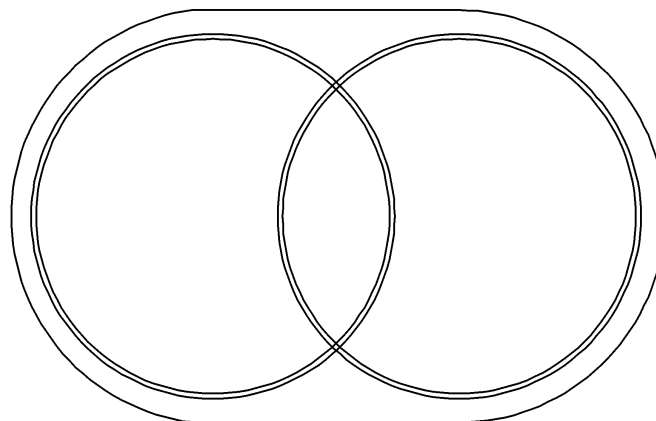


Figure 3: Oblong Double Spiral Configuration

1.4 MULTI-SPIRAL ANALYSIS

Due to the relatively new nature of multi-spiral reinforcement, many computer software models do not include the ability to use interlocking spiral reinforcement in non-circular columns. Caltrans (2015) lists confined concrete equations for both hoop and multi-spiral reinforcement. Esmaeily included Caltrans models for oblong multi-spiral reinforcement in his newest program KSU_RC 2.0 (Esmaeily 2016). Dr. Esmaeily has also developed his own method of compression-tension steel cyclic response that will be included as the method of analysis during the computer software analytical programming portion. The experimental work and analytical studies for development of the original version of the software, KSU_RC, related analytical models, and its progress can be found in Esmaeily (2004, 2005, 2006, 2007).

1.5 OBJECTIVES

This report will investigate several different studies done on the performance of multiple interlocking spirals used as lateral reinforcement in columns with different cross-sectional shapes including: square, rectangular and oblong. Computer programmed analytical modeling done by KSU RC 2.0 (Esmaeily 2016) of a couple different confinement configurations will be assessed and the results will be compared with the experimental investigations done by (Huy 2012), (Yin, Wang and Wang 2012) (Hung, et al. 2012), and (Hung, et al. 2012).

The results compiled in this report will illustrate that multi-spiral reinforcement is a superior choice for reinforced concrete columns.

2. CODES & REQUIREMENTS

2.1 TRANSVERSE REINFORCEMENT

Column ductility greatly depends on the correct amount of lateral reinforcement. Coding requirements address both required confinement area as well as shear strength (ACI 318 2011), (Ou, et al. 2015). Because multi-spiral reinforcement has been studied the most extensively in Southeast Asia, the Ministry of Transportation and Communications in Taiwan, or the MOTC, is also used to provide coding details. In general code requirements are governed by required

confined area. Currently the only codes in the United States that address spiral reinforcement within non-circular columns are those of the California Department of Transportation (Caltrans) Bridge Design Specifications (BDS) and Seismic Design Criteria (SDC) (Li and Belarbi 2011).

The equations used to determine the ratio of confining steel for spiral configurations are denoted by Equation 1 through Equation 6. and Equation 2. The equations for the required area confined by the rectilinear reinforcement shown in Equation 3 and Equation 4. These equations denote design minimums.

$$\rho_s = 0.45 \left(\frac{A_g}{A_c} - 1 \right) \frac{f'_c}{f_y}$$

Equation 1: Volumetric Steel Ratio for Spiral Reinforcement (Caltrans BDS) (MOTC) (ACI 318 2011)

$$\rho_s = 0.12 \frac{f'_c}{f_y} \left(0.5 + \frac{1.25P_e}{f'_c A_g} \right)$$

Equation 2: Volumetric Steel Ratio for Spiral Reinforcement (Caltrans BDS)

$$A_{sh} = 0.3 s_t h_c \frac{f'_c}{f_y} \left(\frac{A_g}{A_c} - 1 \right)$$

Equation 3: Cross-sectional Area of Tie Reinforcement (Caltrans BDS) (MOTC)

$$A_{sh} = 0.12 s_t h_c \frac{f'_c}{f_y} \left(0.5 + \frac{1.25P_e}{f'_c A_g} \right)$$

Equation 4: Cross-sectional Area of Tie Reinforcement (Caltrans BDS)

$$\rho_s = 0.12 \frac{f'_c}{f_y}$$

Equation 5: Volumetric Steel Ratio for Spiral Reinforcement (MOTC)

$$A_{sh} = 0.12 s_t h_c \frac{f'_c}{f_y}$$

Equation 6: Cross-sectional Area of Tie Reinforcement (MOTC)

Equation 1 and Equation 3 are used to address the issue of spalling concrete and the attached loss of strength that can occur. The columns that have been tested evaluated each coding requirement and chose the most conservative numbers. Equation 5 and Equation 6 are ductility equations to address seismic bridge designs.

A_c = Area of confined concrete that measures to the outside diameter of the lateral reinforcement

A_g = Gross area of the section

A_{sh} = Total cross-sectional area of tie-reinforcement within a section that operations within the limits of s_t and h_c

f'_c = Specified compressive strength of concrete

f_y = Specified yield strength of steel reinforcement

h_c = Core dimension of tied column in the direction under consideration

P_e = Axial design load

ρ_s = Ratio of volume of spiral reinforcement to total volume of core concrete

s_t = Vertical spacing of lateral reinforcement

2.2 AXIAL FORCE-MOMENT INTERACTION

The majority of concrete columns experience both axial force and moment force. This combination of forces makes the Force – Moment Diagram necessary to estimate the nominal moment and maximum moment. The research that has been done has used design criteria listed by (ACI 318 2011) (Caltrans BDS 2003) (MOTC 2009). Several of these analytical equations are used by the KSU RC 2.0 computer software (Esmaily 2016).

3. SPECIMENS

The columns investigated in this design have been pulled from several different studies with varying scopes and design criteria. Conversely, each of these columns was designed with the ACI 318, and MOTC codes in mind. To streamline and notate certain column parameters, the following letters are used to express certain attributes: E is experimental while M is modeling; A denotes a square, B denotes a rectangle, and C denotes an oblong shape; lastly, T represents traditional hoops and ties and S represents spirals.

Each set of column design types has varying sizes and strengths of both transversal and longitudinal steel. Along with differing diameter-sized bars, the spiral reinforcement also lists the necessary parameter of the spiral hoop radius. These variations are listed within Section 3.1. The concrete strengths change to some degree between each study and each column specimen and are also addressed. It should also be noted that because of the location of the majority of the experiments, the data is most readily viewable in SI units.

The second set of parameters for the concrete columns, especially under cyclic loading, is the height of the column. Each of these is listed as well in Table 2.

3.1 EXPERIMENTAL CONFIGURATIONS

3.1.1 SQUARE COLUMNS

These types of columns were the first to be subjected to testing regarding interlocking spiral lateral reinforcement. Two designs of rectilinear reinforcement were chosen, as well as three configurations for spiral reinforcement. These designs are shown in Figure 4.

As it is shown in Figure 4, E-A-T1 and E-A-T2 are both shown to have traditional rectilinear reinforcement, but with different layouts and cross transversal reinforcement schemes. Configurations E-A-S1.1 and E-A-S1.2 are very similar except for the radial sizing of the hoops within the column. The last square column layout is the E-A-S2. This figure represents four identical sized interlocking spiral hoops. All of these square type columns are identical in cross sectional size at 60 cm x 60 cm.

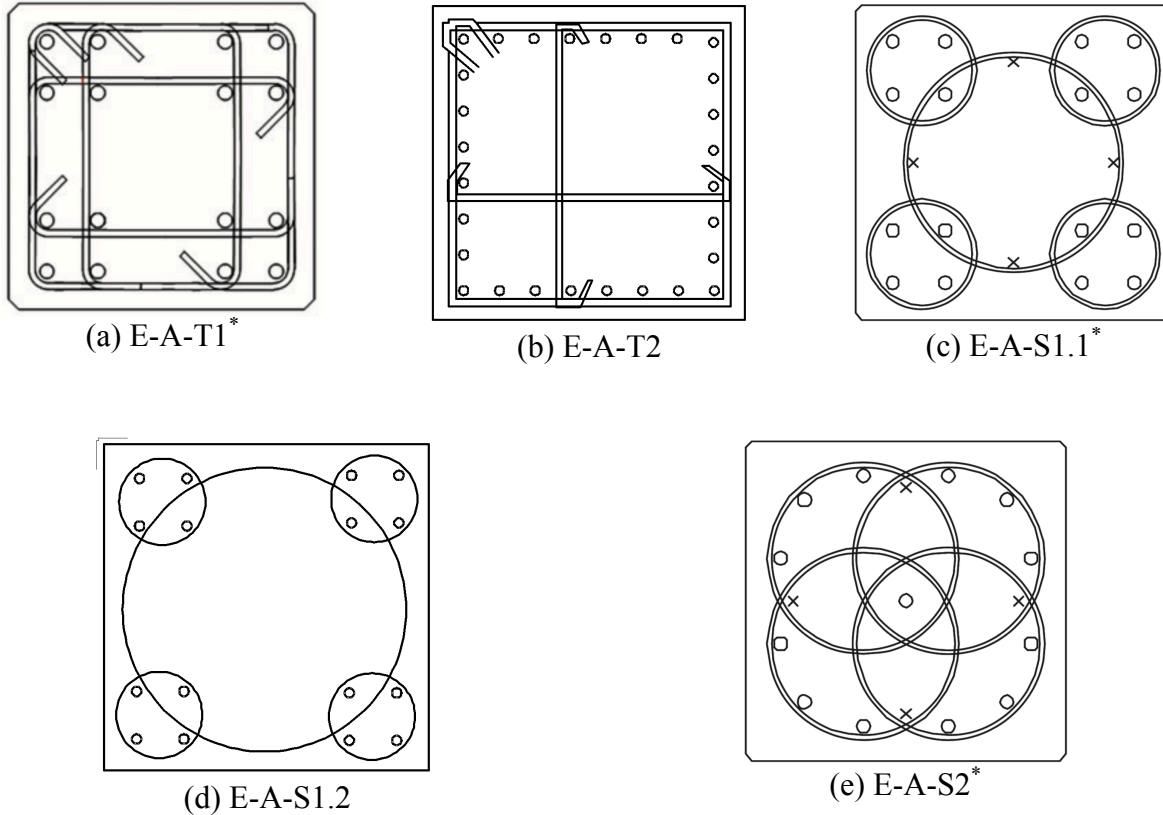


Figure 4: Transverse Reinforcement Configurations for Square Columns

Note: * (Yin, Wang and Wang 2012)

Each of these columns has varying sizes and strengths of both transversal and longitudinal steel. These variations are listed in Tables 1 and 2. The concrete strengths also change to some degree and are also addressed.

3.1.2 RECTANGULAR COLUMNS

Larger rectangular columns have recently been added to the list of tested multi-spiral reinforcement designs. The following rectangular sections include two traditional rectilinear reinforcement layouts, and three multi-spiral reinforcement designs as shown in Figure 5. Every column designed, including those that are oblong in shape, by Ou et al are listed as 60 cm by 87 cm. The remaining two column shapes are larger at 120 cm by 180 cm.

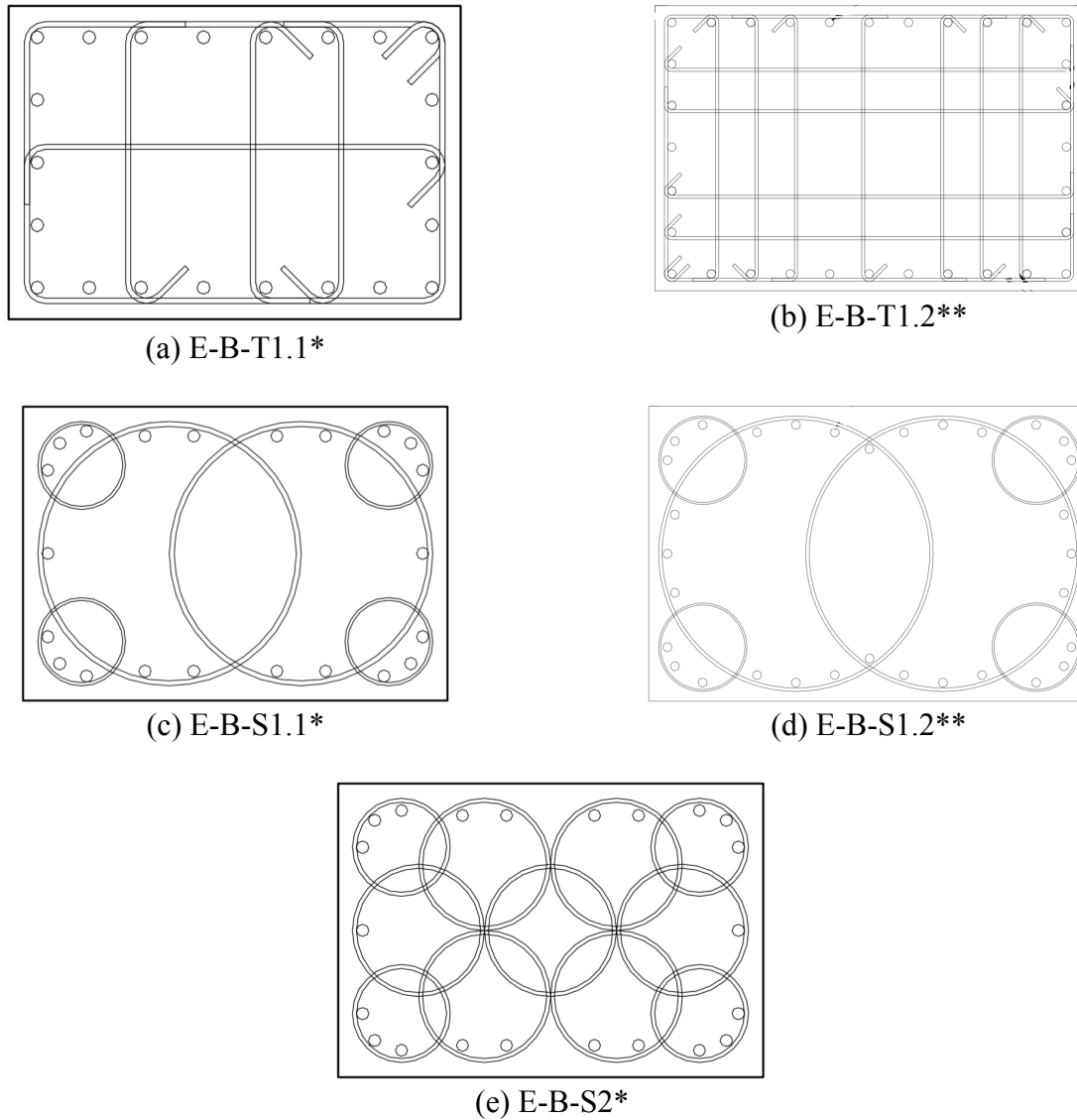


Figure 5: Transverse Reinforcement Configurations for Rectangular Columns

Note: * (Ou, et al. 2015), ** (Hung, et al. 2012)

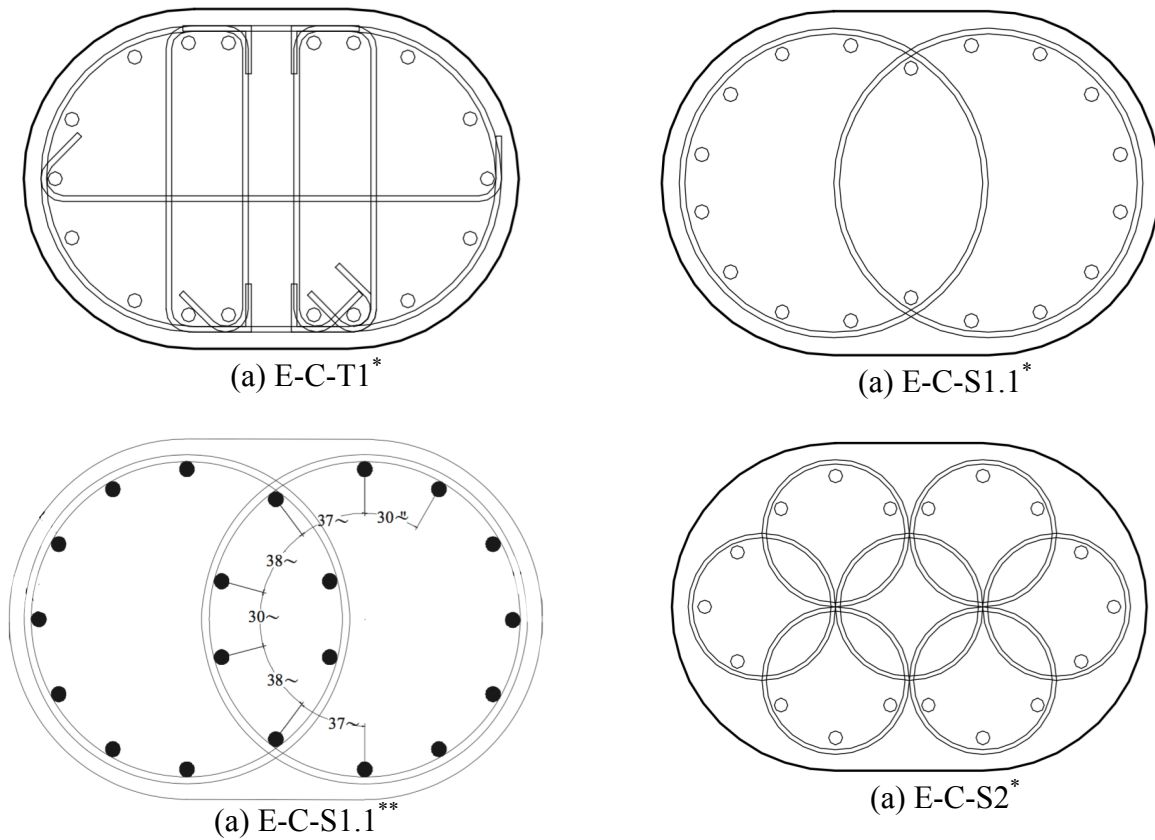
Configuration E-B-T1.1 and E-B-T1.2 are almost identical in layout. However, the column design and experimentation done on the latter was specifically aimed at addressing large sized columns. E-B-S1.1 and E-B-S1.2 are also similarly sized with respect to E-B-T1 and E-B-T2 as these four members were tested alongside the other, respectively. Configuration E-B-S2 is an entirely new layout that introduces a multitude of overlapping spiral transverse reinforcement. Tables 1 and 2 will list the differences in sizes and engineering specifications for all of these members.

3.1.3 OBLONG COLUMNS

The last type of columns to be studied is the oblong shaped column. These types of reinforced concrete cross sections lend themselves well to including spiral design. Ou et al, at this point in time, has done the most comprehensive research on spiral reinforcement in this type of column.

In this paper there will be four oblong column designs discussed. While the oblong shape does increase the usage of multi-spiral transverse reinforcement over traditional rectilinear reinforcement, it also lends itself to simplified designs. The first oblong layout is the only perimeter hoop and tie design. The last three design layouts are combinations of different configurations of transverse spiral reinforcement.

Figure 6: Transverse Reinforcement Configurations for Oblong Columns



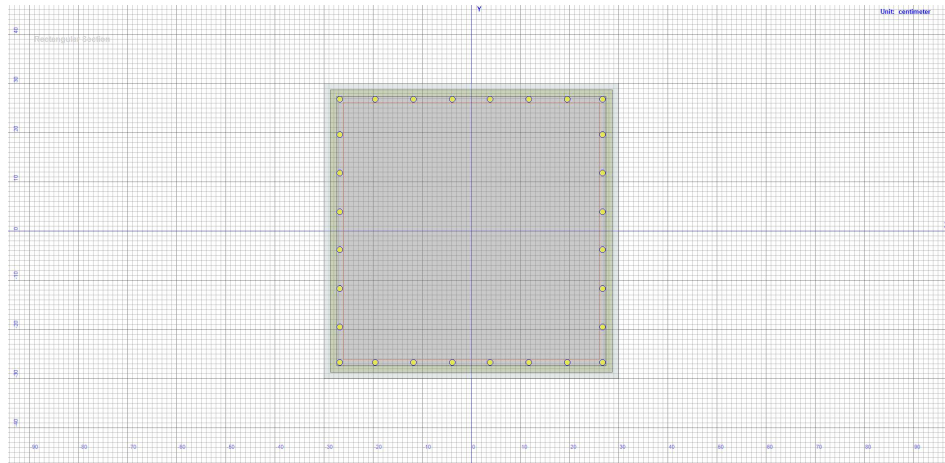
Note: * (Ou, et al. 2015), ** (Hung, et al. 2012)

3.2 COMPUTER ANALYZED LAYOUTS

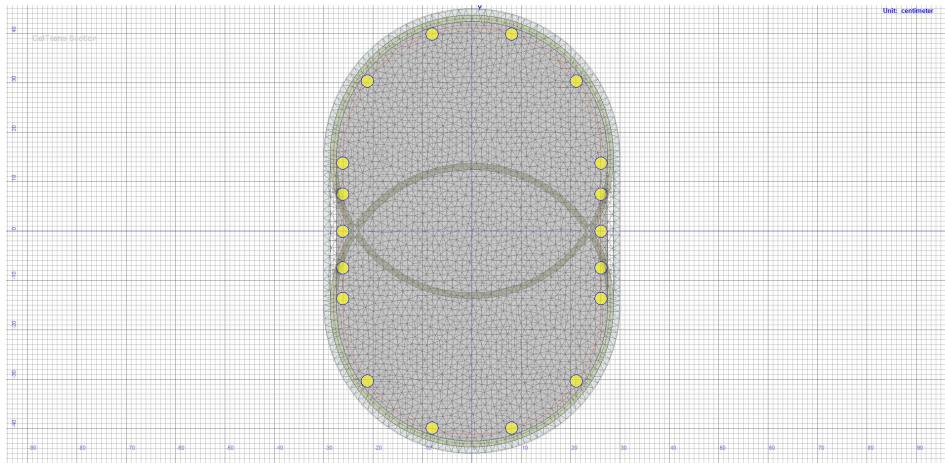
Computer software used to evaluate spiral reinforcement is a new technology. Software modeling tools have become staples of the engineering and construction world. The program KSU RC 2.0 is a software program that has been recently designed to address spiral reinforcement in concrete column cross-sections. Computer programming is continually being reinvented and perfected.

While attempting to model exact replicas of the experimental case studies, it was found that not all constraints could be met. Cross-lateral hoops and ties are as of yet not available in this current program. This lack of interior ties on models decreased the transverse reinforcement ratios, which are definitive in increasing strength and ductility.

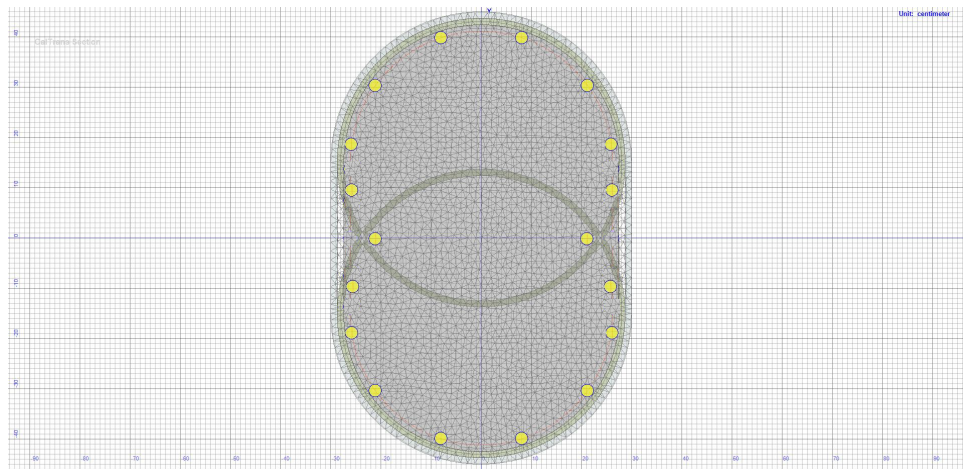
The cross-sections that were attempted by M-A-T2, M-C-T1, and M-C-S1.1 are, respectively, E-A-T2, E-C-T1, and the only current cross-section shape available for spiral reinforcement: E-C-S1.1. These corresponding cross-sections are illustrated in Figure 7. Along with attempting to reproduce the layout conditions, another goal was to replicate the corresponding material properties including concrete strength, transverse steel yield strength and elasticity as well as longitudinal yield steel strength and elasticity.



(a) M-A-T2



(e) M-C-T1



(e) M-C-S1.1

Figure 7: Computer Programmed Transverse Reinforcement Configurations

3.3 MATERIAL PROPERTIES

As this collection of column configurations are pulled from several different studies, it should be noted that there are widely varying specified concrete strengths and yielding steel capacities.

All of the studies performed concrete cylinder compression tests to accurately depict the full 28-day strength of the concrete. The specified concrete compressive strengths for all of the columns fell between 34.4 MPa and 56 MPa. The majority of the columns studied were tested with the 35-40 MPa range. This is due to the current code requirements.

The strength of the steel was chosen to provide correct steel to concrete ratio. The steel strength capacities chosen fell between 250 MPa and 650 MPa. A steel strength of 280 was used for the study done by Yin et al (2012). This was an outlier when compared to the other steel strengths. The majority of the steel strengths were around the 350 to 450 MPa range.

Table 1 shows the configurations of the steel, the corresponding monikers assigned by the researchers, as well as the material properties for each other columns discussed in this paper. The data featured in this table is largely pulled from each researchers' publications. However, Hung, et al. 2012, did not calculate the required steel ratios so these steel ratios were calculated using the codes provided by MOTC and ACI 318.

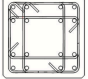
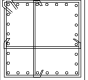
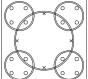
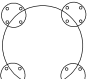
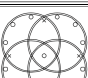
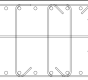
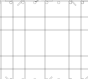


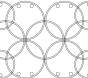

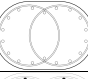
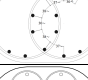

Table 2 details more of the physical layouts of each of the columns. These details include assumed sizes not shown in the research, as well as data pulled from the individual tables. This table also includes the longitudinal reinforcement specifications and ratios.

Table 1: Material Properties I

Column	Cross-Section	Original Name	Concrete		Lateral Reinforcement			ρ_s required	ρ_s provided	
			f'_c (MPa)	f'_{cc} (Mpa)	f'_y (MPa)	Bar Size (mm)				Spacing (mm)
						Small	Large			
E-A-T1		T1/a	34.4	54.2	280	13		85	2.26	2.2
E-A-T2		RC1	41.1	52.9	463	13		90	1.01	1.67
E-A-S1.1		RC2	41.1	59.2	463	10	13	75	1.48	1.25
E-A-S1.2		5S4/h	34.4	57.7	280	13	13	60	1.63	2.05
E-A-S2		4S1/g	34.4	57.6	280	13		75	1.64	2.20
E-B-T1.1		CTR1-MS	47.1	n/a	581	12		75	2.01	2.14
E-B-T1.2		a	n/a	n/a	420	13		90	1.04	1.19
E-B-S1.1		CM1R1-MS	43.1	n/a	581	6	10	60	1.14	1.33
E-B-S1.2		b	n/a	n/a	420	10	16	100	0.73	0.87
E-B-S2		CM2R1-MS	45.5	n/a	648	8	8	60	1.30	1.78
E-C-T1		DTR1-ML	40.9	n/a	581	12		75	2.31	2.73
E-C-S1.1		DM1R1-ML	43.6	n/a	605	10		60	1.04	1.20
E-C-S1.2		B-B	36.2	n/a	454	9		70	0.82	1.32
E-C-S2		DM2R1-MS	56	n/a	648	8		60	1.59	1.56

Note: Data supplied by (Hung, et al. 2012) (Li and Belarbi 2011) (Ou, et al. 2015) (Yin, Wang and Wang 2012)

Table 2: Material Properties II

Name	Cross-Section	Study Name	Side a mm	Side b, mm	A_{g_2} m ²	Spiral D, mm	Height, mm	Longitudinal Reinforcement			
								f_y	Bar Size	Amount	ρ
E-A-T1		T1/a	600	600	0.36	n/a	3000	412	25	16	0.0069
E-A-T2		RC1	600	600	0.36	n/a	1200	430	13	28	0.0033
E-A-S1.1		RC2	600	600	0.36	540, 100*	1200	430	13	28	0.0033
E-A-S1.2		5S4/h	600	600	0.36	420, 210	3000	412	25	16	0.0069
E-A-S2		4S1/g	600	600	0.36	360	3000	412	25	16	0.0069
E-B-T1		CTR1-MS	600	870	0.52	n/a	1800	469	25	22	0.0066
E-B-T2		a	1200	1800	2.16	n/a	8500	420	36	32	0.0048
E-B-S1.1		CM1R 1-MS	600	870	0.52	540, 180	1800	469	25	22	0.0066
E-B-S1.2		b	1200	1800	1.85	3,601, 120	8500	420	36	32	0.0056
E-B-S2		CM2R 1-MS	600	870	0.44	270, 200	1800	469	25	22	0.0077
E-C-T1		DTR1-ML	600	870	0.44	n/a	1800	469	25	18	0.0063
E-C-S1.1		DM1R 1-ML	600	870	0.44	540	1800	469	25	18	0.0063
E-C-S1.2		B-B	610	915	0.48	510	3500	529	25	20	0.0065
E-C-S2		DM2R 1-MS	600	870	0.44	270	1800	469	25	18	0.0063

Note: * numbers not provided by research data. Data provided by (Hung, et al. 2012) (Li and Belarbi 2011) (Ou, et al. 2015) (Yin, Wang and Wang 2012)

4. TESTING SETUP

The testing configurations for the columns were all very similar. Yin et al 2012 and Weng 2006 studied the affects of compressive loading done as a stand-alone force. However, the rest of the studies that have been done have included a more realistic loading set up for high seismic areas including cyclic loading. This type of loading set up provides a more in depth view of the behavior of the columns under different and varying loading patterns.

4.1 AXIAL COMPRESSIVE LOADING

Testing the specimens for axial loading was done using a hydraulic jack. Each study used different specimens, but the set up type is still very similar. These test specimens were set up with linear variable differential transformers (LVDT) to accurately measure the axial strain that occurred during each moment of the testing as shown in Figure 8. The axial testing was done at a steady axial load as prescribed in code.

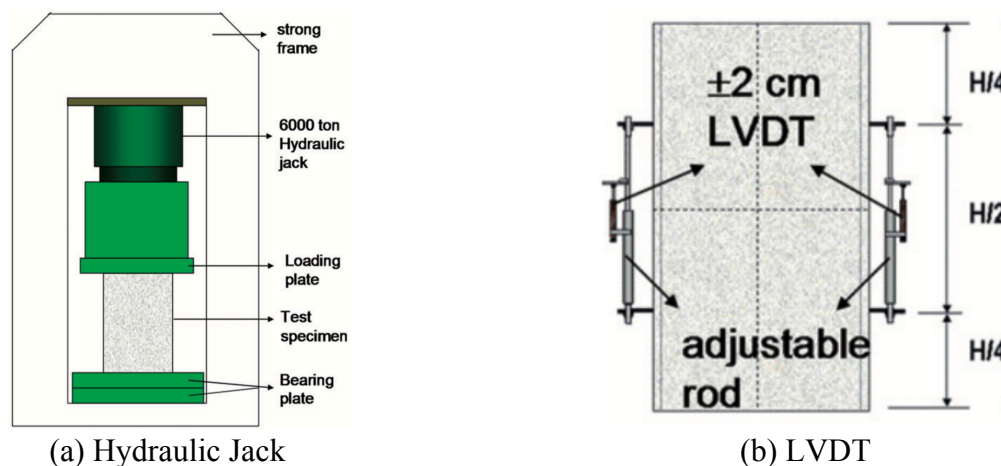
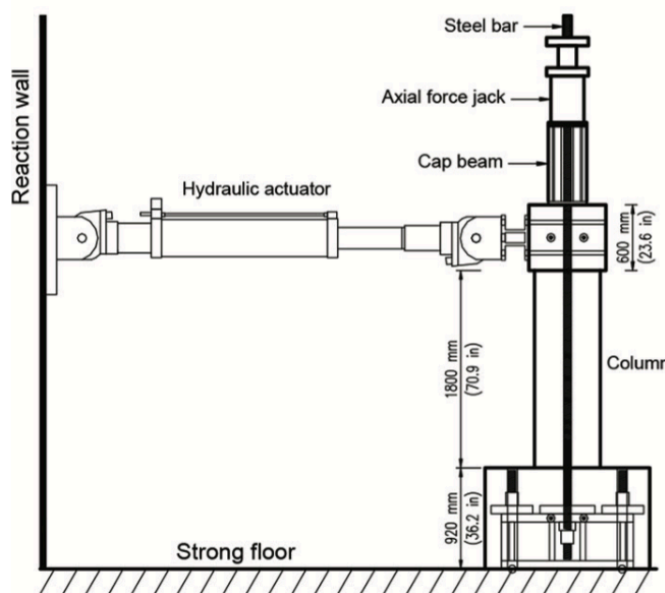


Figure 8: Axial Test Setup (Yin, Wang and Wang 2012)

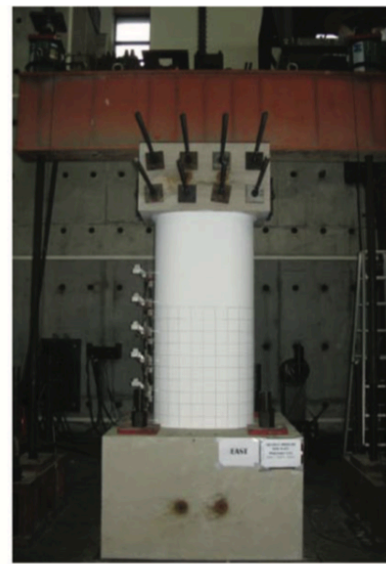
This testing mechanism is standard for the industry. The testing set ups varied in the length of the columns as well as the placement of the LVDT. The specimens were all loaded until failure. These material ruptures were recorded for each column.

4.2 COMBINED AXIAL AND LATERAL CYCLIC LOADING

As with the compressive axial testing, the specimens that were tested were subjected to an axial load using a large hydraulic jack. The largest different between the combined cyclic lateral loading and axially loading is the scope of the testing machines. Another hydraulic jack is added to work in conjunction with a constant axial force application. However, during this application the axial load is set at $0.1A_g f'_c$ while a lateral force is applied in a cyclic fashion. The structural arrangement is shown in Figure 9.



(a) Hydraulic Jack Illustration



(b) Hydraulic Jack Picture

Figure 9: Lateral Hydraulic Jack (Ou, et al. 2015)

The loading was performed in multiple cycles to certain drift ratios. The drift angles or ratios are found from the deflection at the application of the lateral point to load to the center of the box above the column height to the middle of the foundation box located the floor. Displacement was controlled during the testing using hydraulic actuators set to read the drift at levels of $\pm 0.25\%$, $\pm 0.375\%$, $\pm 0.5\%$, $\pm 0.75\%$, $\pm 1\%$, $\pm 1.5\%$, $\pm 2\%$, $\pm 3\%$, $\pm 4\%$, $\pm 6\%$, $\pm 8\%$, and $\pm 10\%$ (ACI 374 n.d.)

Figure 10 illustrates an additional column tested by Li and Belarbi for large-scale applications and the testing done by Ou et al.

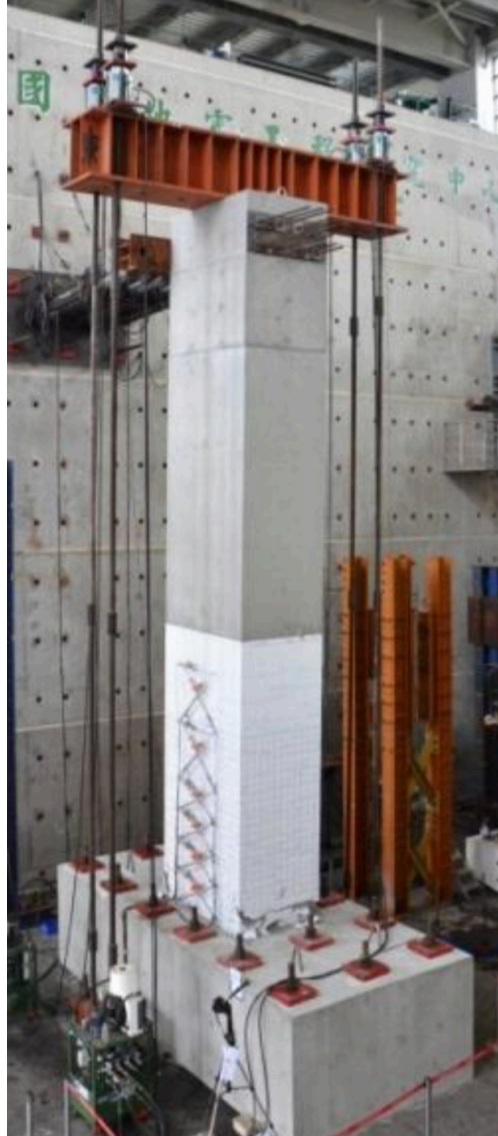


Figure 10: Lateral Hydraulic Jack and LVDT (Hung, et al. 2012)

The cyclic loading was performed through drift levels with repeated cycles. With each cycle the degradation of the columns including cracking, spalling, failure of lateral reinforcement steel as well as longitudinal reinforcement of steel. The loading conditions in one study produced an extra moment caused by the P-delta affect, which needed to be addressed to accurately express the applied moment.

4.3 COMPUTER CROSS-SECTIONS

The computer software analysis provided with KSU RC 2.0 allowed approximating the real world conditions carried out during the experimental investigations (Esmaily 2016). The program is able to run Axial Force Deflection, Moment Curvature and Lateral Force Deflection analysis using several different methods produced by different professionals including Dr. Asad Esmaily. An issue incurred was the inability to use spiral reinforcement for rectangular columns. Thusly, the modeled columns were the traditionally rectilinear reinforcement configurations. However, the oblong column configurations were able to be very closely replicated for both the traditional hoop and tie reinforcement as well as the newer multi-spiral reinforcement.

For the Force Deflection calculations and computer analysis, the number closest coinciding with the experimental data was used. Esmaily's first method was chosen for the calculations and computer analysis regarding the Force Deflection diagram. There are options to choose several different coding types for the Axial Moment Force diagram. The chosen method was ACI 318. This was expected to illustrate most accurately the experimental results.

5. TEST RESULTS

5.1 AXIAL RESULTS

The failure modes of the columns are illustrated as examples in Figure 11. The conventional perimeter hoop and ties failed by the complete failure of the cross ties by separation or rupture. This failure mode led to further buckling of the longitudinal reinforcement. The columns that were reinforcement with the multiple interlocking hoops experienced severe spalling, however, the lateral reinforcement maintained for the entire duration of the test. The spiral hooping experienced fracturing and moderate buckling cause by the significant dilation of the concrete. These results are fairly homogenous across all of the axially loaded samples.



(a) E-A-T1



(b) E-A-S1.2

Figure 11: Axial Failure Examples (Yin, Wang and Wang 2012)

Figure 12 displays the stress-strain relationships of each set of columns subjected to an axial load. E-A-T1 and E-A-S1.1 are higher in nominal strength and that could misrepresent the data.

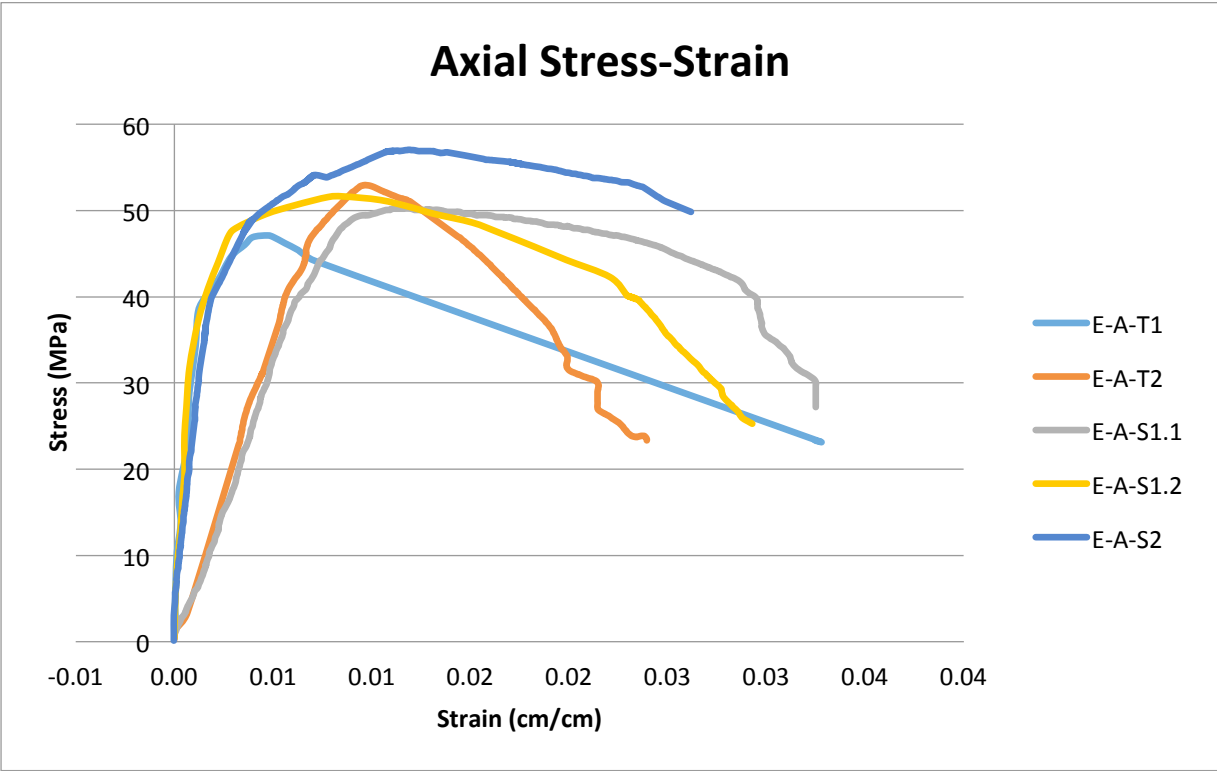
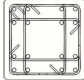
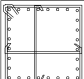
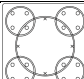
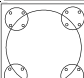
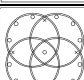



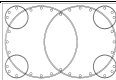
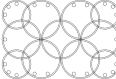


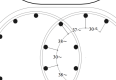
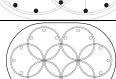


Figure 12: Axial Stress - Strain Diagram

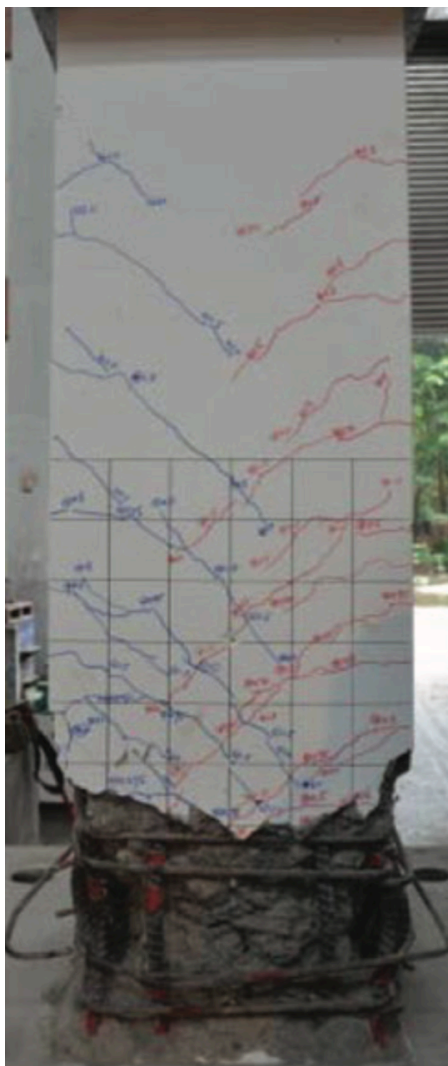
Table 3: Steel Reduction Ratios

Shape	Column	Layout	ρ_s	Ratio
Square	E-A-T1		2.2	1.00
Square	E-A-T2		1.67	0.76
Square	E-A-S1.1		1.25	0.57
Square	E-A-S1.2		2.05	0.93
Square	E-A-S2		2.20	1.00
Rectangle	E-B-T1.1		2.14	1.00
Rectangle	E-B-T1.2		1.19	0.56
Rectangle	E-B-S1.1		1.33	0.62
Rectangle	E-B-S1.2		0.87	0.41
Rectangle	E-B-S2		1.78	0.83
Oblong	E-C-T1		2.73	1.00
Oblong	E-C-S1.1		1.20	0.44
Oblong	E-C-S1.2		1.32	0.48
Oblong	E-C-S2		1.56	0.57

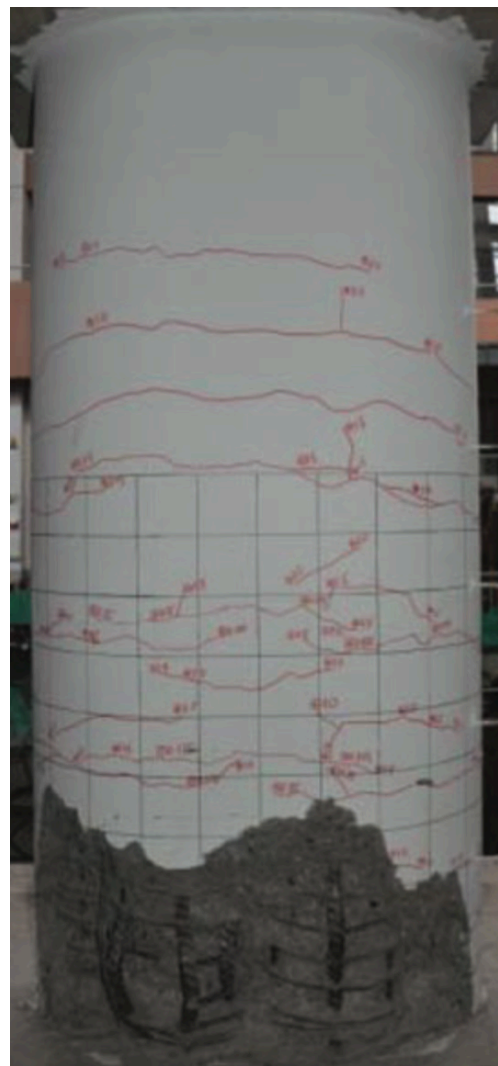
*Note: The first row of each shape is the standard against which each steel ratio is compared.

5.2 COMBINED AXIAL AND CYCLIC LOAD RESULTS

The failure modes of the columns are illustrated as examples in Figure 14. Very similarly to the axial loading test specimens, the conventional perimeter hoop and ties failed by the complete failure of the cross ties by separation or rupture. This led to further buckling. The columns that were reinforcement with the multiple interlocking hoops experienced severe spalling, however; only the specimen E-C-1.1 experienced complete rupturing of lateral reinforcement. The spiral hooping in the remainder of these columns experienced fracturing and moderate buckling caused by the significant dilation of the concrete.



(a) E-B-T1



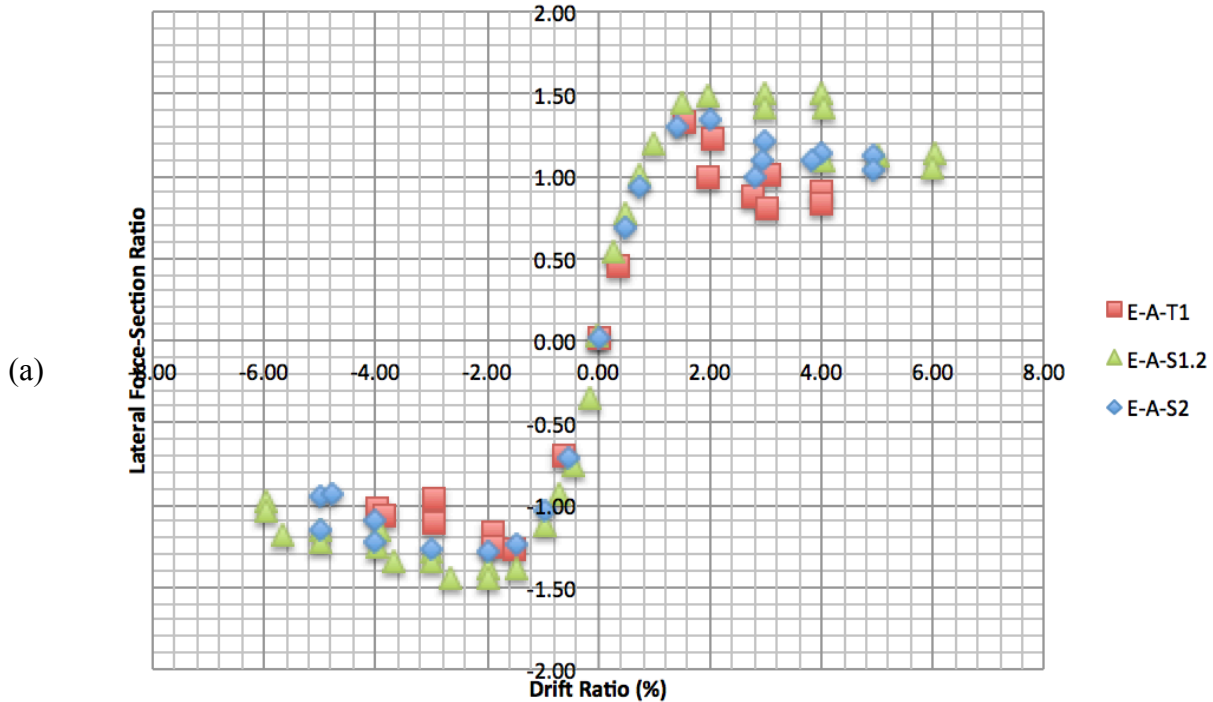
(b) E-C-S2

Figure 13: Axial Failure Examples (Ou, et al. 2015)

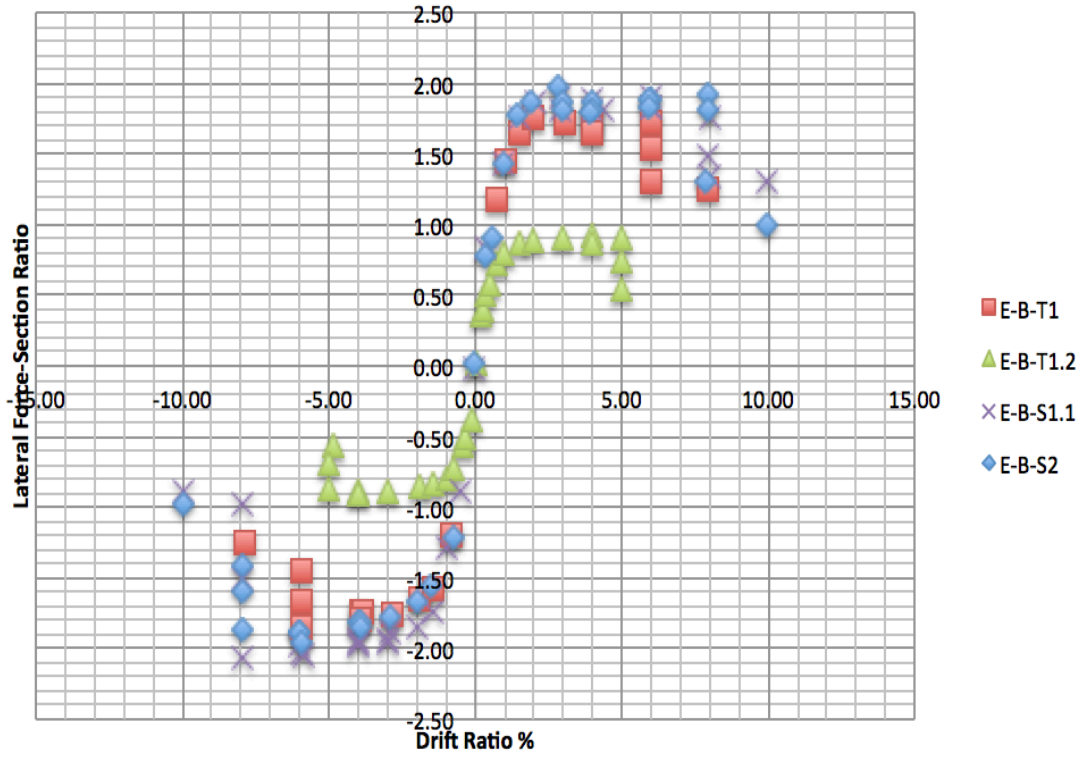
The LDVT set up collected the data throughout the test to model each of the hysteresis loops. To keep the pictures simple, the graphs have been simplified to unmodified hysteresis envelopes. Additionally, because the columns were from different studies and performed differently, a factor was used to compare different sized sections. The lateral forces were changed to a lateral force-section ratio to make comparison across the studies simpler. Figure 14 shows these hysteresis envelope graphs categorized by shape.

The hysteresis loops can be used to illustrate the ductility factor. The ultimate yield is idealized and represents the correct drift angle that corresponds with the highest strength. This drift ratio is divided by the ultimate drift angle to produce the ductility of the column, (Ou, et al. 2015). The ductility values for E-B-T1, E-B-S2, E-C-T1 and E-C-T2 are 6.10, 6.54, 7.40, and 8.71 respectively.

The drift angles for all of the spiral-reinforced columns exceeded the drift angles for the traditional rectilinear reinforcement designs.



(b)



(c)

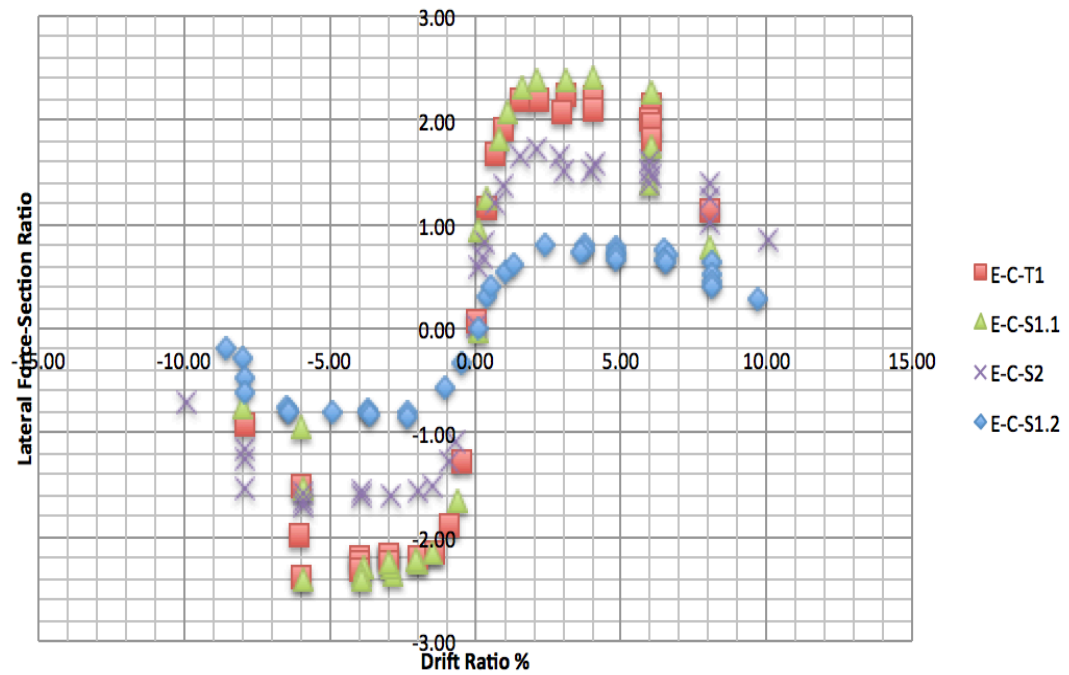


Figure 14: Hysteresis Envelopes

5.3 COMPUTER PROGRAM ANALYSIS

While the KSU RC 2.0 program currently does not have an option for multi-spiral reinforcement in rectangular sections, the oblong columns were very easily analyzed within the program. The Caltrans model oblong column shapes greatly outperformed the square columns for the simple ACI 318 Force-Moment analysis. To make the comparisons more homogenous, Force was converted into Stress. This would rectify the differences in strength due to cross-sectional areas. Figure 15 illustrates the differences between the plain square rectilinearly reinforced column when compared to both the traditionally laterally reinforced oblong column, as well as the spiral lateral reinforced oblong column. The multi-spiral column and the traditionally laterally reinforced column analyses were very similar. The spiral cross-section performed slightly higher in maximum moment.

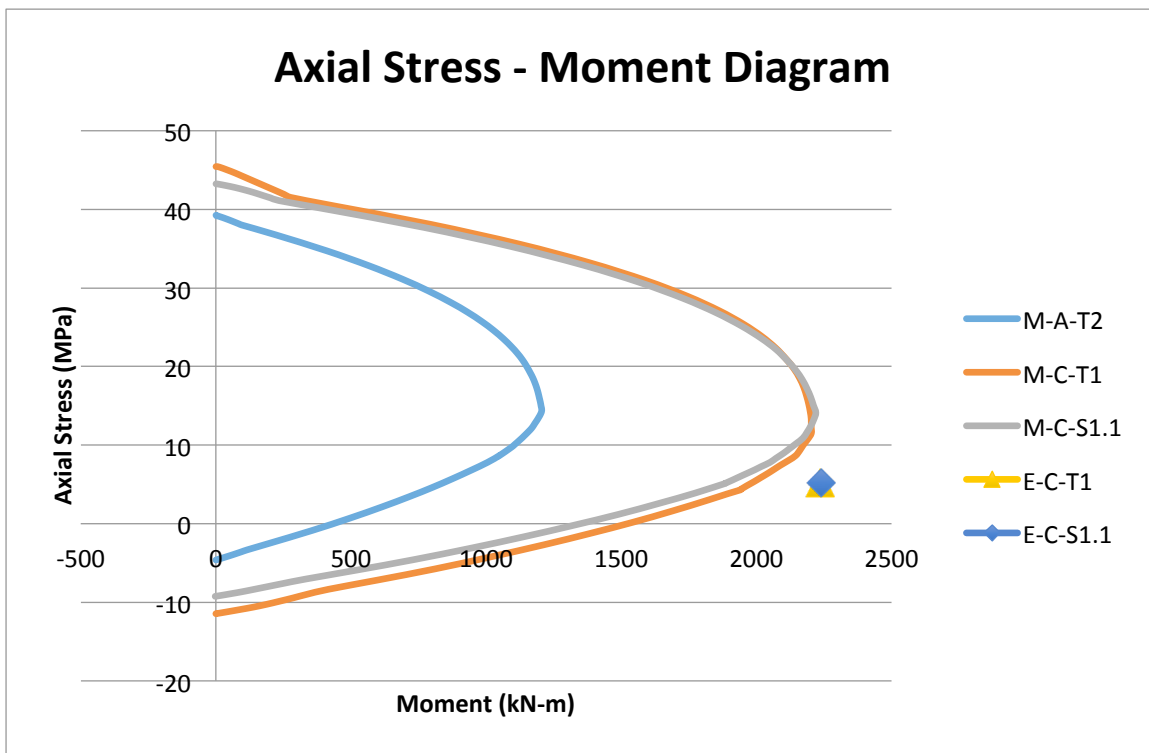


Figure 15: Axial Stress - Moment Computer Model Diagram (Including Experimental Results for two of the cross-sections)

Figure 16 illustrates the second analysis done by the program: Lateral Stress-Deflection. This assimilates force applied laterally that causes deflection in the lateral direction. The deflections for the oblong columns were taken in the long direction. KSU RC 2.0 provides the data for lateral deflection in centimeters (Esmaeily 2016). As with the previous analysis, the numbers were altered to more accurately represent and compare the data with the experimental results.

Again, the oblong columns both greatly outperformed the square column. The traditional hoop and tie reinforced column cross-section showed a higher lateral stress, but with less deflection before rupture when compared with the multi-spiral reinforcement.

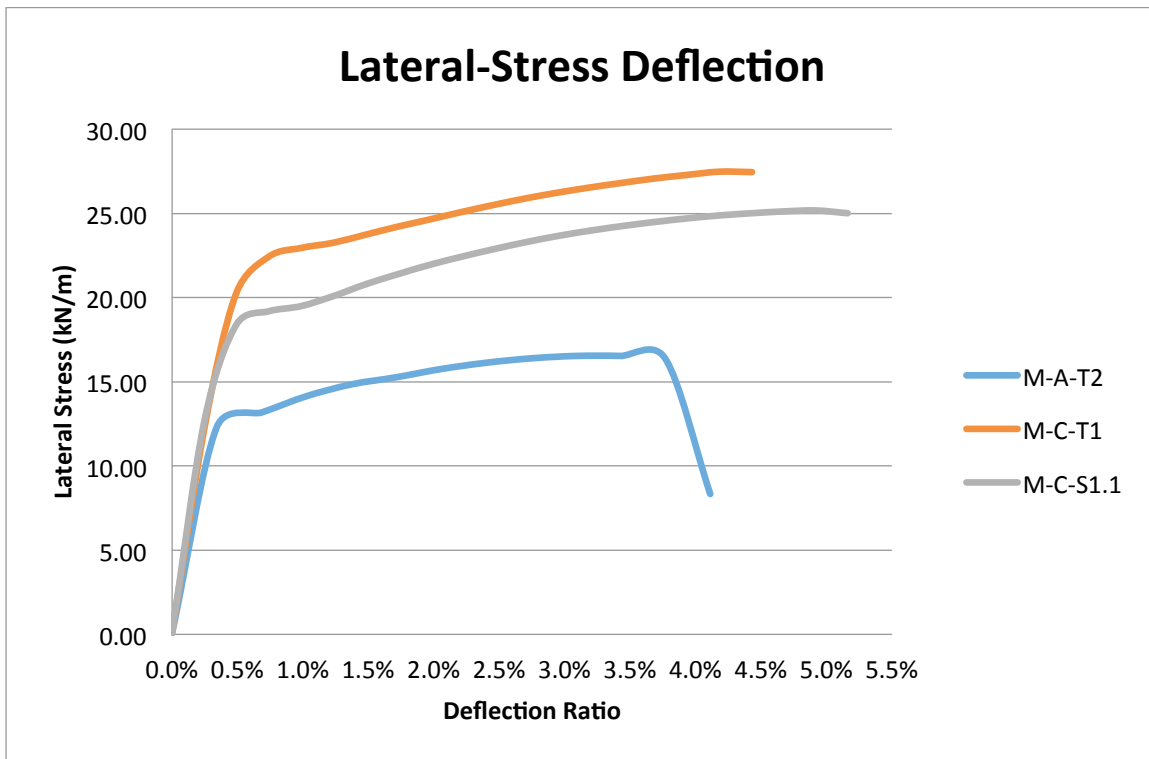


Figure 16: Lateral Stress - Deflection Diagram

The last analysis done by the program is the Moment-Curvature Analysis as shown in Figure 17. As with the previous analyses, the oblong column cross-sections performed very similarly. The maximum bending moment for the multi-spiral instance is the greatest. The square

column shape specimen had a significantly lower maximum bending moment with a higher moment curvature.

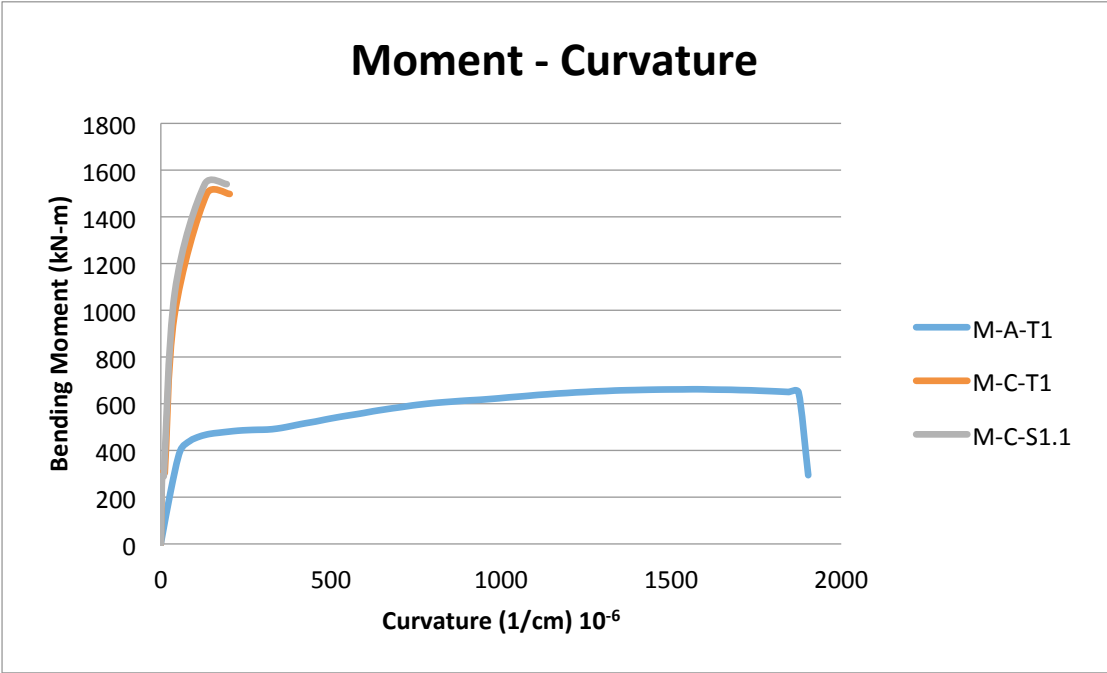


Figure 17 - Moment - Curvature Diagram

6. EXPERIMENTAL & COMPUTER ANALYSIS COMPARISON

6.1 AXIAL STRESS – BENDING MOMENT

There were only two comparable shapes to make a comparison with the experimental data versus the computer-analyzed data. These two shapes were the oblong cross-sections with both the traditional rectilinear reinforcement and the multi-spiral reinforcement.

For the experiments the maximum bending moments were almost identical. However, it should be noted that both experimental values performed outside of the bending moment diagram loop. These maximum moments are shown in Figure 15.

6.2 LATERAL FORCES

While the comparisons are more difficult to make, the hysteresis loops shown in Figure 14 can be compared to the Lateral Stress-Deflection Diagram. Figure 16 shows the computer analysis results for the deflection ratios for M-A-T2 dropped strongly at 3.8%. The deflection ratio for M-C-T1 showed rupture at approximately 4.4%. The highest deflection ratio was that of M-C-S1.1 at 5.2%.

As shown in Figure 14, the comparison of the two traditional hoop and tie reinforced column types are very similar between the experiment data and the program analysis at approximately 4%. However, with the oblong columns these numbers are significantly lower than the experimental data provided in Figure 14 against the similar types of cross-sections. The experimental data for both the oblong columns show approximately a 3% increased when compared with the analytical data.

7. CONCLUSIONS AND RECOMMENDATIONS

Five square columns were tested under axial forces alone, three square columns, five rectangular columns and four oblong columns were tested under combined axial compression and lateral cyclic loads. These columns had multiple types of lateral reinforcement including multiple interlocking spirals as well as multiple conventional rectilinear lateral reinforcement.

Computer analysis using KSU RC 2.0 was performed with similar cross sections for three of the experimental columns. These column cross-sections were a traditional rectilinear hoop square, a traditional hoop and tie oblong, and a two spiral oblong cross-section.

7.1 EXPERIMENTAL DATA

Every column tested performed in a ductile manner and achieved necessary strengths. The best performing oblong spiral reinforced column achieved 19% higher ductility than the traditional perimeter hoop and tie oblong column. At first glance it would seem that axial strength was not greatly improved, but the allowed strain was significantly increased while also maintaining higher compressive strengths throughout the loading process. Further, of the multi-spiral reinforcement designs contain fractions that almost reach 50% of confining steel when compared to the traditional rectilinear designs.

The spiral reinforced square columns achieved 30% higher drift angle than the matching rectilinearly reinforced square column. This multi-spiral reinforced column contained just 76% of the steel that the rectilinear column contained.

The rectangular shaped columns did not achieve as drastic of differences in ductility in strength, however, the multi-spiral designs still improved on the traditional rectilinear configuration. Along with improving the ductility, the design steel was reduced by 45%. In large-scale construction processes, it could prove extremely beneficial.

7.2 KSU RC 2.0

The first conclusion is that oblong columns perform better in axial stress, bending moment, and ductility than rectangular columns. The oblong column cross-section results for these analyses also showed slight disparities with the experimental results suggesting that multi-

spiral reinforcement could perform even better than the provided analytical models currently available.

The Force-Moment diagram (that was adjusted to the illustration in Figure 15) indicates that multi-spiral reinforcement will perform better in ductility. The allowable moment is larger, but the axial forces are lower. It should be noted that, despite the small differences, the multi-spiral reinforced section contained 44% of the lateral steel as compared to the traditionally laterally reinforced section. This is a dramatic difference that suggests clear superiority.

7.3 RECOMMENDATIONS

7.3.1 MULTI-SPIRAL REINFORCEMENT

Because the results are so outstanding and quantifiable, it would be worthwhile for the industry to further examine the beneficial affects of using multi-spiral reinforcement for the transverse steel as opposed to the traditional rectilinear reinforcement. This type of reinforcement could allow for less steel, which equates to less money. These results also illustrate that due to the higher ductility, columns using multi-spiral reinforcement could be the most beneficial lateral reinforcement type for seismic areas.

7.3.2 COMPUTER SOFTWARE

More equations are being investigated and invented to accurately analyze the confining affects of spiral reinforcement. These new equations should be modeled and compared to the experimental data. Computer software is an invaluable tool and a large part of the construction industry, and it would be beneficial to add more designable constraints for this type of software to more accurately represent experimental data.

REFERENCES

- ACI 318. "Building Code Requirements for Structural Concrete." *American Concrete Institute*, 2011: 503.
- ACI 374. "Acceptance Criteria for Moment Based on Structural Testing and Commentary." *American Concrete Institute* 1-5.
- Ahmad, S.H., and S.P. Shah. "Complete triaxial stress– strain curves for concrete ." *ASCE Journal of the Structural Division* 108, no. 4 (1982): 728-742.
- Caltrans. *California Department of Transportation*. 2015.
<http://www.dot.ca.gov/des/techpubs/manuals/bridge-design-practice/page/bdp-21.pdf>
(accessed 2016).
- Caltrans BDS. "Bridge Design Specifications." *California Department of Transportation*, 2003: 8-1 to 8-58.
- Darwin, D., and D.A. Pecknold. "Nonlinear biaxial stress–strain law for concrete ." *ASCE Journal of the Engineering Mechanics Division* 103, no. 2 (1969): 229-241.
- Esmaily, A. "KSU_RC 2.0, a software to analyze flexural performance of reinforced concrete sections and columns." 2016. <http://www.ce.ksu.edu/faculty/esmaeily> (accessed 2016).
- Esmaily, A., Peterman, R. (2007). "Performance Analysis Tool for Reinforced Concrete Members", *Journal of Computers & Concrete*, October 2007, Vol.4, No. 5, Pp 331-346
- Esmaily, A., Lucio K. (2006). "Analytical Performance of Reinforced Concrete Columns using Various Confinement Models", *ACI SP-238-6*, pp-95-110
- Esmaily, A., Xiao, Y. (2005). "Behavior of Reinforced Concrete Columns under Variable Axial Loads: Analysis", *American Concrete Institute, ACI Structural Journal*, Vol. 102, No. 5, Pp. 736-744, September-October 2005
- Esmaily, A., Xiao, Y. (2004). "Behavior of Reinforced Concrete Columns under Variable Axial Loads", *American Concrete Institute, ACI Structural Journal*, Vol.101, No.1, pp.124-132, January-February 2004
- Hung, H.H., P.H. Wang, Y.L. Yin, J.C. Wang, and K.C. Chang. "Large-scale Cyclic Loading Test on a Multi-Spiral Stirrup Bridge Pier Constructed by Automated Method." *15 WORLD CONFERENCE ON EARTHQUAKE ENGINEERING*. Lisbon, 2012.
- Huy, N.S. "Cyclic Behavior of Oblong and Rectangular Bridge Columns with Conventional Tie and Multi-Spiral Transverse Reinforcement ." Department of Construction Engineering, National Taiwan University of Science and Technology, Taiwan, 2012.
- Kupfer, H., H.K. Hilsdorf, and H. Rusch. "Behavior of concrete under biaxial stress." *ACI Journal Proceedings* 66, no. 8 (1969): 656-666.
- Li, Qian, and A. Belarbi. "Seismic Behavior of RC Columns with Interlocking Spirals under Combined Loadings Including Torsion ." *The Twelfth East Asia-Pacific Conference on Structural Engineering and Construction* . Elsevier Ltd , 2011. 1281-1291.
- Mander, J.B., M.J.N. Priestly, and R. Park. "Theoretical stress–strain model for confined concrete." *ASCE Journal of Structure Engineering* 114, no. 8 (1988): 1804-1846.
- MOTC. "Seismic Bridge Design Specifications." *Ministry of Transportation and Communications*, 2009: (in Chinese).

- Ou, Y.C., S.H. Ngo, R. Hwasung, S.Y. Yin, J.C. Wang, and P.H. Wang. "Seismic Performance of Concrete Columns with Innovative Seven- and Eleven-Spiral Reinforcement ." *ACI Structural Journal*, 2015: 579-591.
- Pantazopoulou, S.J. "Detailing for reinforcement stability in RC members ." *ASCE Journal of Structure Engineering* 124, no. 6 (1998): 623-632.
- Shah, S.R., A. Fafitis, and R. Arnold. "Cyclic loading of spirally reinforced concrete ." *ASCE Journal of Structure Engineering* 109, no. 7 (1983): 1695-1710.
- Sheikh, S.A., and M.T. Toklucu. "Reinforced concrete columns confined by circular spirals and hoops." *ACI Structural Journal* 90, no. 5 (1993): 542-553.
- Shirmohammadi, F., Esmaeily, A. (2016), "Software for Biaxial Cyclic Analysis of Reinforced Concrete Columns", TechnoPress, Journal of Computers and Concrete, Vol. 17, No. 3 (2016) 000-000, DOI: <http://dx.doi.org/10.12989/cac.2016.17.3.000>
- Fatemeh Shirmohammadi, Asad Esmaeily, (2015) "Performance of Reinforced Concrete Columns under Bi-axial Lateral Force/Displacement and Axial Load", Elsevier Journal of Engineering Structures, ENGSTRUCT-D-14-01700R2, Aug. 2015
- Tanaka, T.H., and R. Park. "Behavior of axially loaded concrete columns confined by elliptical hoops." *ACI Structural Journal* 96, no. 6 (1999): 967-971.
- Weng, C.C., Y.L. Yin, J.C. Wang, C.Y. Liang, and C.M. Huang. "Experimental investigation on rectangular SRC columns with multi-spiral confinements." *4th International Conference on Earthquake Engineering*. Taipei: ICEE, 2006.
- Yin et al. "Experimental studies of rectangular columns with innovative spiral confinements." *17th KKCNN symposium on civil engineering, Bangkok*. Bangkok, 2004.
- Yin, Samuel Yen-Liang, Jui-Chen Wang, and Ping-Hsuing Wang. "Development of multi-spiral confinements in rectangular columns for construction automation." *Journal of the Chinese Institute of Engineers* 35, no. 3 (2012): 309-320.